

RESEARCH

Open Access



The regulatory subunit MoB56 of PP2A phosphatase regulates pathogenicity, growth and development in a protein complex with the atypical catalytic subunit Ppg1 in the rice blast fungus *Magnaporthe oryzae*

Rui-Jin Wang^{1,2} , Danrui Cui¹, Rui Zhao¹, Yujie Jin¹, Wenhui Zeng¹, Ye Yang¹, Linlu Qi¹, Lihui Xiang¹ and You-Liang Peng^{1*}

Abstract

Protein phosphatase 2A (PP2A) is usually a heterotrimeric enzyme, consisting of a catalytic subunit (C) and a scaffolding subunit (A) associated with a third, variable regulatory subunit (B). Fungi usually carry a single gene for A and C subunits, and three genes for the B subunit. In addition, fungi contain a conserved atypical C subunit named Ppg1, which is essential to the pathogenicity of the rice blast fungus *Magnaporthe oryzae*. However, it remains largely unknown how the B subunit combinatorically assembles with the A and C subunits or Ppg1 to regulate fungal growth, development and pathogenicity. Here we report and functionally characterize one regulatory subunit of PP2A, named MoB56, in *M. oryzae*. We generated a *MoB56* deletion mutant $\Delta mob56$, which was severely defective in vegetative growth, conidiation and septum formation, and had lost pathogenicity. The defects of $\Delta mob56$ could be rescued by introducing *MoB56* fused with *GFP* (*MoB56-GFP*) at its C terminus. Fluorescence microscopic observations revealed that the MoB56-GFP signals were widely distributed in the cytoplasm and formed a dot-like structure at the center of the septum in conidia, appressoria and infection hyphae, supporting its function in septation. Further, we performed co-immunoprecipitation and pull-down assays, indicating that MoB56 forms a protein complex with the A subunit and Ppg1 in mycelial cells. The yeast two-hybrid assay showed that MoB56 could interact with the A subunit of PP2A but not with Ppg1, while Ppg1 could interact with the A subunit, suggesting that the A subunit ties MoB56 with Ppg1 for the protein complex formation. In addition, we revealed that MoB56 has multiple isoforms, which are likely originated from alternative splicing and sumoylation. This is the first report revealing that the regulatory subunit B56 is associated with the PP2A-like phosphatase Ppg1 in fungi. Importantly, this study showed that B56, like Ppg1, is essential to the pathogenicity of *M. oryzae*, offering a potential new lead to control this devastating fungal pathogen by targeting specific PP2A-like phosphatase. Together, this study provides important information for understanding how the regulatory subunit B56 of PP2A regulates fungal pathogenicity and for the control of rice blast disease.

Keywords Rice blast fungus, Pathogenicity, PP2A-like phosphatase, Regulatory subunit B56, Ppg1

*Correspondence:

You-Liang Peng
pengyl@cau.edu.cn

¹ MARA Key Laboratory of Pest Monitoring and Green Management, College of Plant Protection, China Agricultural University, 100193 Beijing, China

² MARA Key Laboratory of Surveillance and Management for Plant Quarantine Pests, College of Plant Protection, China Agricultural University, 100193 Beijing, China



© The Author(s) 2023. **Open Access** This article is licensed under a Creative Commons Attribution 4.0 International License, which permits use, sharing, adaptation, distribution and reproduction in any medium or format, as long as you give appropriate credit to the original author(s) and the source, provide a link to the Creative Commons licence, and indicate if changes were made. The images or other third party material in this article are included in the article's Creative Commons licence, unless indicated otherwise in a credit line to the material. If material is not included in the article's Creative Commons licence and your intended use is not permitted by statutory regulation or exceeds the permitted use, you will need to obtain permission directly from the copyright holder. To view a copy of this licence, visit <http://creativecommons.org/licenses/by/4.0/>.

Background

Dynamic phosphorylation of proteins reversibly controlled by protein kinases and phosphatases is a fundamental process regulating cell division, growth and differentiation, and cellular responses to environmental signals (Hunter 1995). In eukaryotes, many genes encode protein kinases that catalyze protein phosphorylation on serine/threonine residues, but only a limited number of genes encode serine/threonine protein phosphatases for protein dephosphorylation. Protein phosphatase 2A (PP2A) is a major phosphatase family in eukaryotic cells and usually functions as a heterotrimeric complex consisting of a catalytic subunit (C) and a scaffolding subunit (A) associated with a third, variable regulatory subunit (B) (Shi 2009; Cohen 2010; Ghosh et al. 2014). The complex structure and regulation system of PP2A represents a highly conserved signal transduction system present in diverse organisms, from yeasts to humans. In mammalian cells, there exist two genes encoding each of the catalytic subunits and the scaffolding subunit, and more than fifteen genes for the B regulatory subunits that can be further classified into four subfamilies (B/B55, B'/B56, B''/B72 and B'''/striatin) (Kiely and Kiely 2015). The variety and comprehensive functions of the B subunits, and their various temporal and spatial distribution make them a determinant factor for full activity and substrate specificity of PP2A (Virshup and Shenolikar 2009).

Fungi possess three to four regulatory subunits for PP2A that belong to the B55, B56 and Striatin subfamilies (Healy et al. 1991; Jiang and Hallberg 2000; Kück et al. 2016; Shu et al. 1997), and lack the B72 subfamily. Compared to mammals and plants, fungi usually have only one member for each of the three B subfamilies (Booker and DeLong 2017). The three B subunits subfamilies in fungi display distinct roles even in the same biological process. In *Saccharomyces cerevisiae*, the *cdc55* mutant displays abnormally elongated buds, decreased growth rate and increased sensitivity to cold, while the *rts1* mutant is sensitive to elevated temperatures and accumulates glycogen (Healy et al. 1991; Shu et al. 1997; Wilson et al. 2002). In *Aspergillus nidulans*, *parA* (B56) or *pabA* (B55) deletion leads to a severe defect in mycelial growth. The $\Delta parA$ mutant had a hyperseptation phenotype, whereas the $\Delta pabA$ mutant had a delayed-septation defect, suggesting that *parA* and *pabA* counteract function for septum formation (Zhong et al. 2014). *parA* and *pabA* also differ in their subcellular localizations (Zhong et al. 2014). In *Neurospora crassa*, the regulatory subunits RGB1 and B56 are required for proper growth and development (Shomin-Levi and Yarden 2017), while Striatin involved in the striatin-interacting phosphatase and kinase (STRIPAK) complex is important for fruiting body formation and hyphal fusion (Kück et al. 2016). These

lines of evidence further support the distinct functions and target specificities of regulatory subunits in model fungi.

The regulatory subunits have also been reported in some pathogenic fungi (Shin et al. 2013; Kück et al. 2016; Beier et al. 2016; Han et al. 2019; Qiu et al. 2021). In *Candida albicans*, both *Cdc55* and *Rts1* are known to be important in growth, morphogenesis, and virulence, but they play distinct roles in the processes (Han et al. 2019). In the maize pathogen *Fusarium verticillioides*, deletion of the B56 subunit results in a severe defect in virulence (Shin et al. 2013). In *Sordaria macrospora*, the STRIPAK complex has been reported to govern fungal sexual development (Beier et al. 2016). In addition, the B55 subunit is known to be important in the phytopathogenic oomycete *Phytophthora sojae* (Qiu et al. 2021). However, functional characterization of the regulatory subunits of PP2A phosphatases in plant pathogenic pathogens is limited. It remains largely unknown how each of the B subunits combines with the subunits A and C or Ppg1 to regulate pathogenicity, growth and development in plant pathogenic fungi.

Magnaporthe oryzae is a filamentous ascomycete that causes the rice blast disease, the most devastating disease of cultivated rice worldwide (Dean et al. 2012). It is also a model fungus to study plant–fungi interactions whose whole genome has been sequenced (Dean et al. 2005; Xue et al. 2012). From the whole genome sequence, it has been known that *M. oryzae* has a single gene each for the typical C and scaffold A subunits of PP2A, which are highly similar to the Pph21/Pph22 (Sneddon et al. 1990) and ScTpd3 (Vanzyl et al. 1992) in *S. cerevisiae*, respectively. *M. oryzae* has three genes for the B regulatory subunits that belong to B55, B56 and Striatin subfamily. In addition, the pathogen carries one PP2A-like catalytic subunit MoPpg1 that is orthologous to ScPpg1 in *S. cerevisiae* (Posas et al. 1993). However, to date, only MoPpg1 has been functionally characterized (Du et al. 2013). Functions and regulatory mechanisms of PP2A in *M. oryzae* remain largely to be elucidated.

Here we report the functional characterization of the regulatory subunit MoB56 in *M. oryzae*. Our results indicate that MoB56 is important for septum formation, growth and conidia morphology and is essential for pathogenicity. We also showed that MoB56 is widely distributed in the cytoplasm but forms a dot-like structure at the center of the septum. Further, we revealed that MoB56 forms a complex with the A subunit and MoPpg1 via direct interaction with the A subunit. This is the first report demonstrating the relationship of the B56 subunit with Ppg1 in fungi, and it will be informative to understand how the Ppg1 PP2A-like phosphatase regulates fungal pathogenicity.

Results

Deletion of the regulatory subunit encoding gene *MoB56*

Previous studies reported that the regulatory subunit B56 of PP2A is important for septation and cytokinesis, conidiation and virulence in yeast and some filamentous fungi (Dobbelaere et al. 2003; Vargas-Muñiz et al. 2016). These functions of B56 are similar to those regulated by the PP2A-like phosphatase C subunit MoPpg1 in *M. oryzae* (Du et al. 2013), suggesting that B56 may work with MoPpg1 in *M. oryzae*. To identify the B56 subunit in *M. oryzae*, we performed pBLAST against the *M. oryzae* 70-15 genome by using the amino acid sequences of regulatory subunit Rts1 in *S. cerevisiae* and B56 in *Homo sapiens* as queries, resulting in the identification of MGG_12130 as the B56 ortholog in *M. oryzae*, which was designated as MoB56. Sequence alignment of MoB56 with its orthologs in yeasts, filamentous fungi, *Arabidopsis thaliana*, *Caenorhabditis elegans* and *H. sapiens* showed that MoB56 contains the major characters of B56 regulatory subunit that has 8 HEAT-like domains, with very divergent N- and C-termini (Fig. 1a and Additional file 1: Figure S1). To functionally characterize *MoB56*, we

constructed a knockout vector for the gene based on the homologous replacement strategy (Fig. 1b) and successfully generated a knockout mutant $\Delta mob56$ in the P131 strain background that was verified by PCR (Fig. 1c) and Southern blot assay (Fig. 1d).

MoB56 is important for growth and conidiation, and regulates conidium morphology and septation in *M. oryzae*.

To investigate the biological function of MoB56 in *M. oryzae*, we compared the vegetative growth and conidiation phenotypes of $\Delta mob56$ with that of the wild-type (WT) strain P131 and the complementary strain cMoB56. The results showed that $\Delta mob56$ displayed severe defects in vegetative growth and conidiation (Fig. 2). Compared to P131, $\Delta mob56$ formed much smaller and flatter colonies (Fig. 2a–c), which had fewer aerial mycelia (Fig. 2b), and rarely generated conidia on conidiophores (Fig. 2d), resulting in the conidia production of $\Delta mob56$ accounting less than 1% of P131 (Fig. 2e). The complementary strain cMoB56 completely recovered all the mentioned defects.

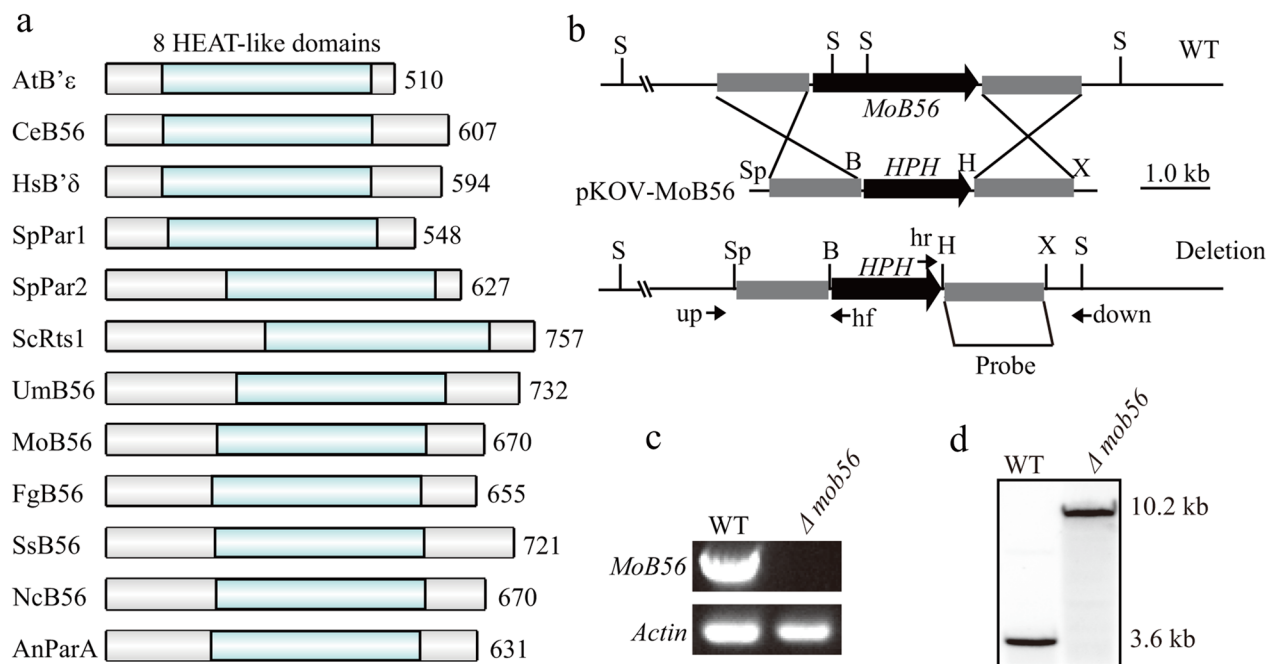


Fig. 1 Deletion of *MoB56* in *Magnaporthe oryzae*. **a** Comparison of conserved domain diagrams among the regulatory B56 ortholog protein sequences in selected species. NCBI accession numbers are as follows: *Arabidopsis thaliana* epsilon isoform of B56, AtB'ε, NP_001030770.1; *Caenorhabditis elegans* CeB56, NP_001122845.1; delta isoform of B56 from *Homo sapiens*, HsB'δ, KAI2542369.1; *Schizosaccharomyces pombe* SpPar1, NP_588206.1; *S. pombe* SpPar2, NP_593298.1; *Saccharomyces cerevisiae* ScRts1, NP_014657.1; *Ustilago maydis* UmB56, XP_011389548.1; *M. oryzae* MoB56, XP_003719828.1; *Fusarium graminearum* FgB56, XP_011324500.1; *Sclerotinia sclerotiorum* SsB56, XP_001591242.1; *Neurospora crassa* NcB56, XP_961132.2; *Aspergillus nidulans* ParA, XP_868849.1. **b** Gene deletion strategy of *MoB56* in *M. oryzae*. Restriction enzymes used for constructing the pKOV-MoB56 replacement vector are labeled by *Bam*HI (B), *Spe*I (Sp), *Hind*III (H) and *Xho*I (X). **c** PCR amplification of *MoB56* gene in the wild-type (WT) and knockout strains. **d** Southern blot assay of $\Delta mob56$, genomic DNA of the wild-type and mutant strains were digested with *Sac*I (S) as shown in **b**

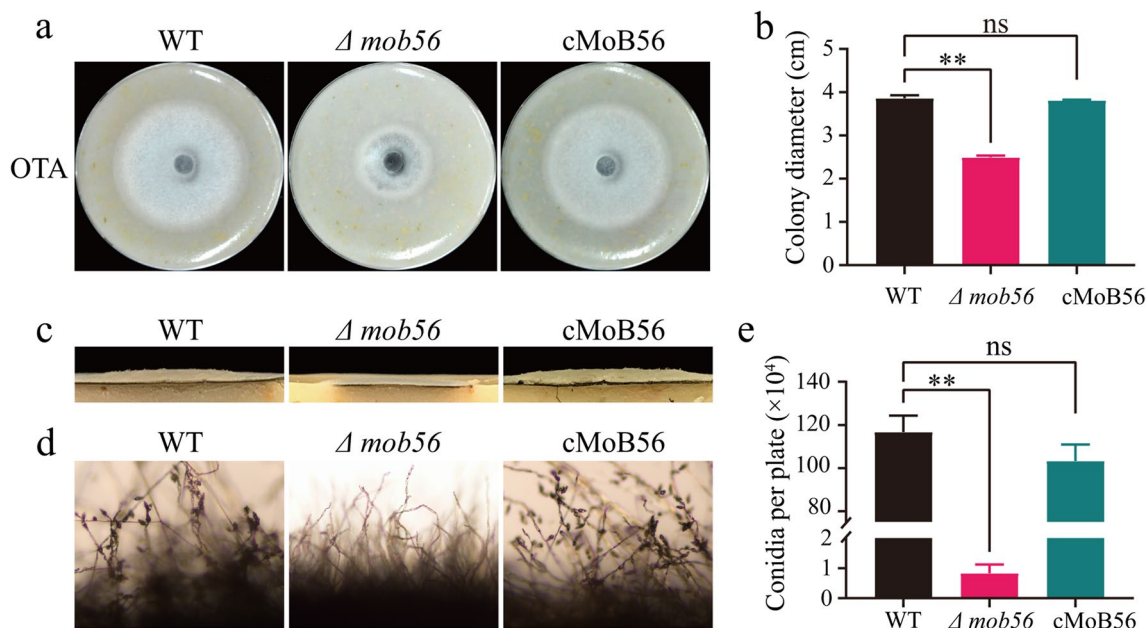


Fig. 2 MoB56 is required for mycelial growth and conidiation in *Magnaporthe oryzae*. **a** Colony morphologies of the wild-type (WT) strain, the $\Delta mob56$ deletion mutant and the complementary strain cMoB56 grown on an OTA plate at 28°C for 5 days. **b** Colony diameters of the indicated strains. **c** Aerial hyphal growth of the indicated strains. **d** Conidiophore development of the indicated strains. **e** Statistical analysis of conidial numbers of the indicated strains grown on OTA plate at 28°C for 7 days. Error bars represent \pm SD. **, $P < 0.01$

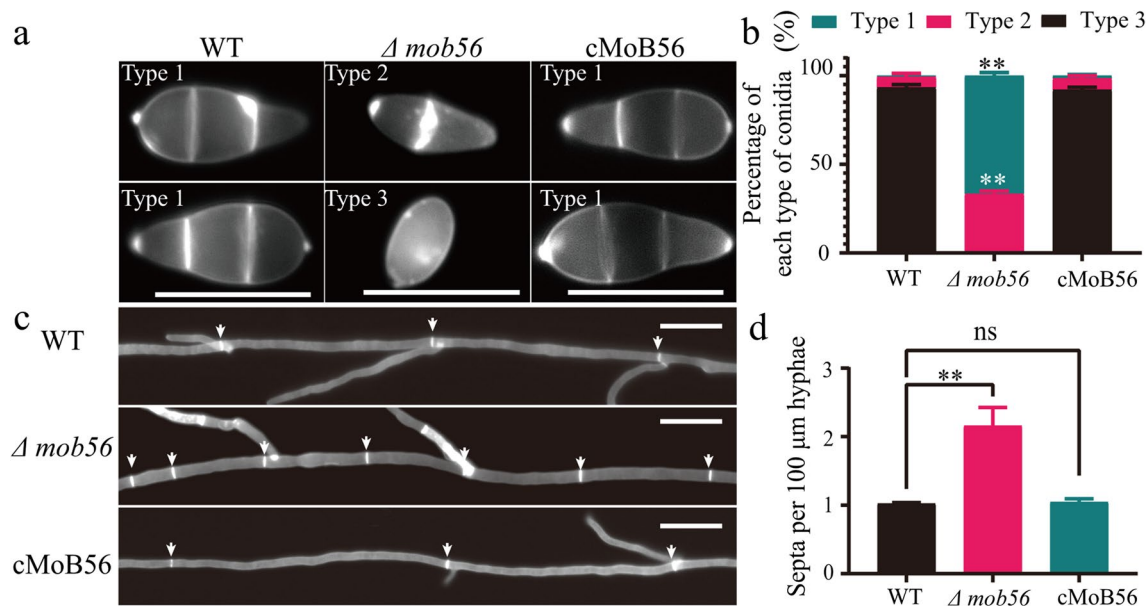


Fig. 3 MoB56 regulates conidium morphology and septation in *Magnaporthe oryzae*. **a** Conidia of the $\Delta mob56$ deletion mutant and the complementary strain cMoB56 were stained with Calcofluor white (CFW) and examined by epifluorescence microscopy. Bars = 20 μm. **b** Percentage of different types of conidia generated by the indicated strains. Error bars represent \pm SD. **, $P < 0.01$ **c** Hyphae of the indicated strains were stained with CFW and examined by epifluorescence microscopy. Bars = 20 μm. **d** Statistical analysis of the number of septa per 100 μm of hyphae in the indicated strains. Error bars represent \pm SD. **, $P < 0.01$

We further microscopically assessed the septation in the conidia and mycelia of $\Delta mob56$ with the Calcofluor white staining (CFW staining) assay. As shown in Fig. 3, conidia produced by $\Delta mob56$ were much smaller than those produced by P131 (Fig. 3a), and contained only one or two cells (Fig. 3b), whereas over than 90% of the P131 conidia carried three cells separated by two septa (Fig. 3b). In mycelia, $\Delta mob56$ produced more septa than P131 (Fig. 3c). The number of septa per 100 μm hyphae of $\Delta mob56$ was almost twice that of P131 (Fig. 3d). The results indicate that the B56 subunit plays critical roles in regulating septation and conidium morphology.

MoB56 is essential to the pathogenicity of *M. oryzae*.

We further performed spray- and wound-inoculation assays to test the role of *MoB56* in pathogenicity. Compared to the successful infection of P131 and complementary strains, $\Delta mob56$ failed to infect both the barley leaves (Fig. 4a, d) and the wounded rice seedling (Fig. 4b, e), indicating that the $\Delta mob56$ mutant lost pathogenicity. We then investigated the infection-related development of $\Delta mob56$ and found that although most conidia of $\Delta mob56$ were able to germinate, with 86.4% germination rate at 8 h post-inoculation (hpi) (Fig. 4c, f), the germinated conidia rarely elaborated appressoria (Fig. 4c, g).

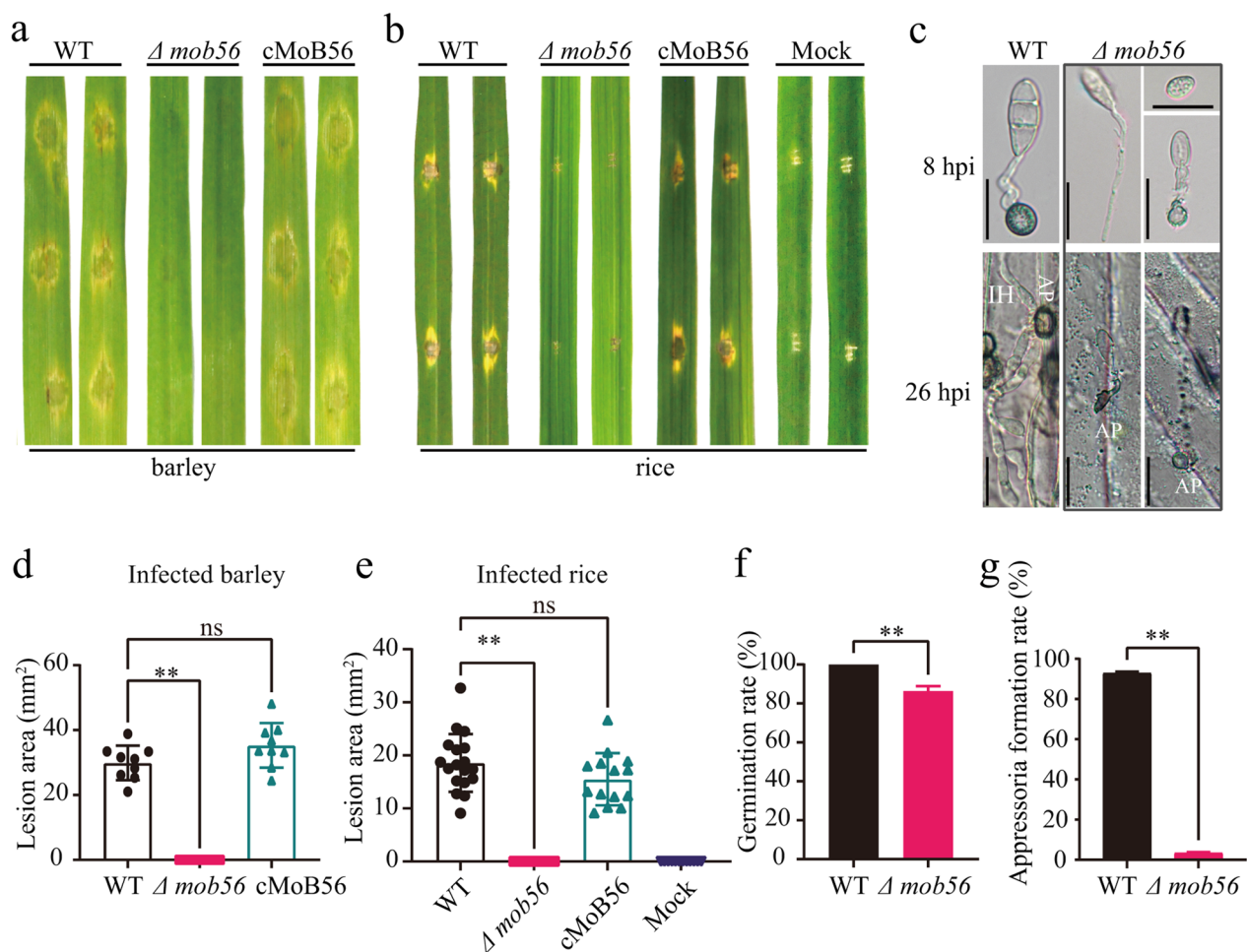


Fig. 4 MoB56 is essential to the pathogenicity of *Magnaporthe oryzae*. **a** Pathogenicity test on unwounded barley leaves. One-week-old barley seedlings were inoculated with conidial suspensions of WT, the $\Delta mob56$ mutant and its complemented strain cMoB56. Photographs were taken at 5 days post-inoculation (dpi). **b** Pathogenicity test on wounded rice leaves. Detached rice leaves of four-week-old rice seedlings were inoculated with the mycelia of the indicated strains. Photographs were taken at 5 dpi. **c** The infection-related development process observation of the indicated strains on hydrophobic coverslips at 8 h post-inoculation (hpi) and on barley epidermal cells at 26 hpi. Bars = 20 μm . **d** Statistical analysis of each lesion area on barley leaves. Error bars represent \pm SD. **, $P < 0.01$. **e** Statistical analysis of each lesion area on wounded rice seedling leaves. Error bars represent \pm SD. **, $P < 0.01$. **f** Statistical analysis of germination rate of the indicated strains on hydrophobic coverslips after 8 hpi. Error bars represent \pm SD. **, $P < 0.01$. **g** Statistical analysis of appressorium formation rate of the indicated strains on hydrophobic coverslips after 12 hpi. Error bars represent \pm SD. **, $P < 0.01$

g). The rarely produced appressoria of $\Delta mob56$ failed to penetrate the barley leaves even at 26 hpi (Fig. 4c). These results demonstrate that the B56 subunit of PP2A is essential to the pathogenicity of *M. oryzae*.

MoB56-GFP signals form a dot-like structure at the septum

To better understand how the B56 subunit functions in *M. oryzae*, we investigated the subcellular distribution of MoB56 at different growth and development stages by generating a construct in which GFP was fused to the C-terminus of MoB56 and transforming it into $\Delta mob56$. As expected, *MoB56-GFP* rescued all the phenotypic defects in $\Delta mob56$. We then picked up one of the transformants for epifluorescence microscopic observation of MoB56-GFP. As shown in Fig. 5, the signals of MoB56-GFP were widely distributed in the cytoplasm of conidia, germ tubes, appressoria, infection hyphae and mycelia. Interestingly, a dot-like structure with conspicuously stronger MoB56-GFP signals was observed at the center of the septum in conidia (Fig. 5a, b), appressoria (Fig. 5c), infection hyphae (Fig. 5d) and mycelia (Fig. 5e). The specific dot-like structure of MoB56-GFP observed at the septum in mycelia, conidia, appressoria and infection

hyphae further supported that MoB56 functions in septum formation.

MoB56 has multiple variants and interacts with the scaffold subunit A in a protein complex containing Ppg1 in mycelial cells

Because the phenotypic defects of $\Delta mob56$ were similar to that of the $\Delta moppg1$ mutant (Du et al. 2013), we reasoned that MoB56 might interact with MoPpg1 that is a PP2A-like catalytic subunit. However, yeast two-hybrid assay (Y2H) indicated that MoB56 could not directly interact with MoPpg1 in yeast cells (Fig. 6a). We then assumed that MoB56 may indirectly interact with MoPpg1 via a protein complex and performed tandem affinity purification and mass spectrometry (TAP-MS) analysis of the Ppg1-precipitated proteins. The analysis indicated that MoB56 and the scaffold subunit A (PP2Aa) were among the Ppg1-precipitated proteins (Fig. 6b). To confirm the result, we also performed a co-immunoprecipitation (Co-IP) assay, using a transformant of the P131 strain expressing MoB56-3HA and MoPpg1-3Flag. The assay showed that MoB56-3HA could be co-immunoprecipitated with MoPpg1-3Flag (Fig. 6c). However, multiple bands were detected in total protein extracts and the

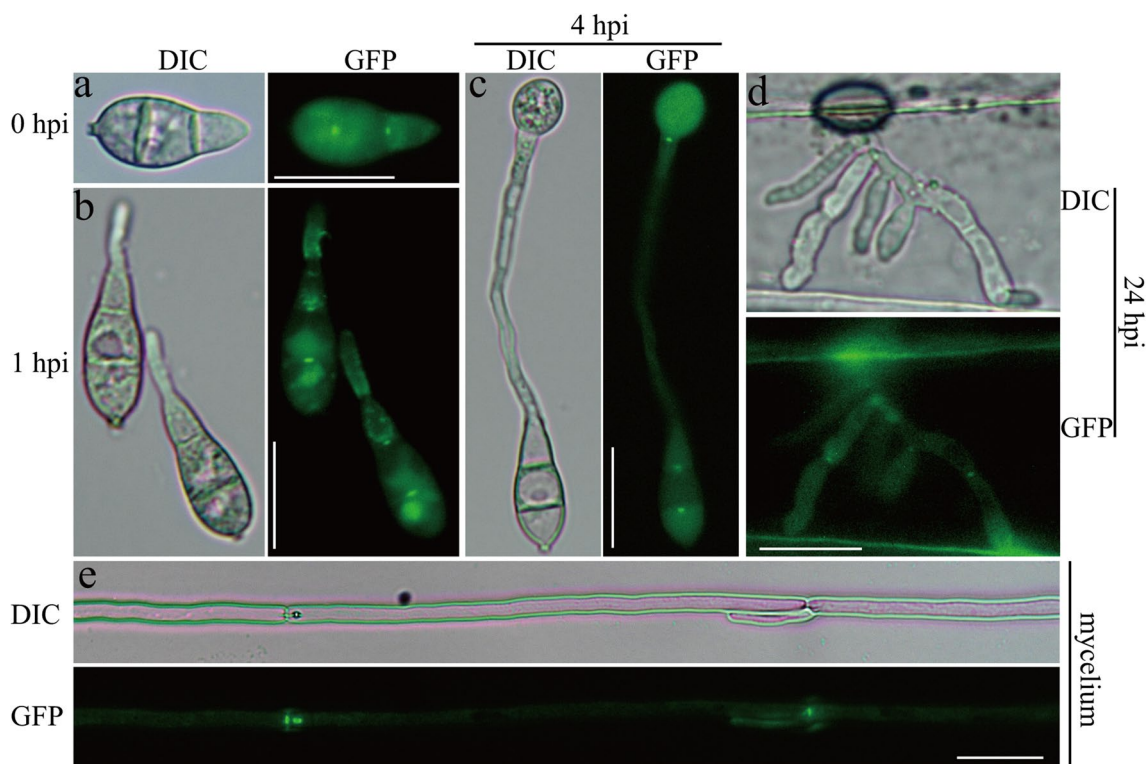


Fig. 5 Subcellular localization of MoB56-GFP in *Magnaporthe oryzae*. MoB56-GFP distributes into the cytoplasm and explicitly assembles as a dot-like structure in the center of septa in mycelia, conidia, primary appressoria and infection hyphae. Assembly of MoB56-GFP in conidia was observed at 1 h post-inoculation (hpi). Bars = 20 μ m

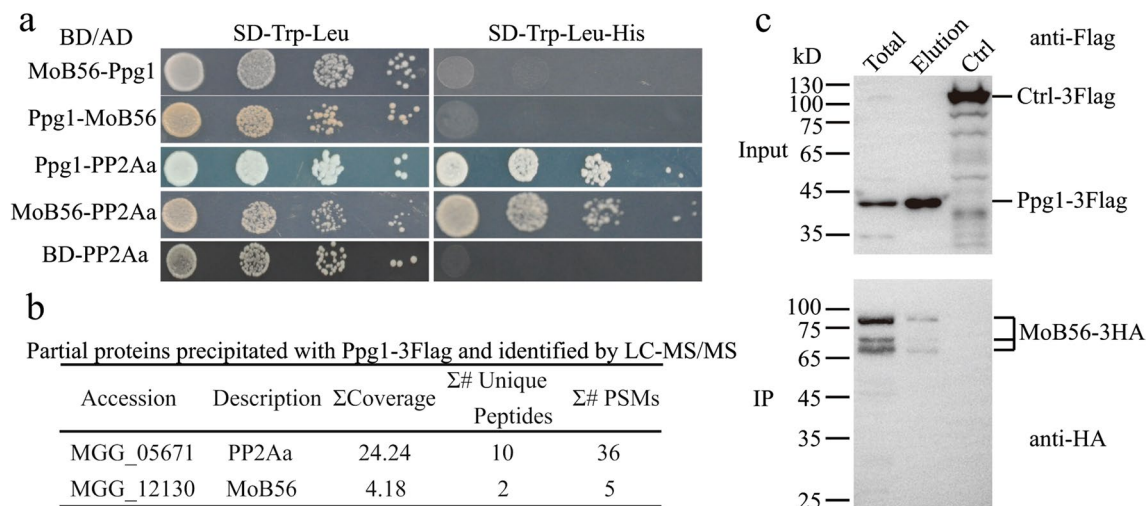


Fig. 6 Interaction assay of MoB56 with the scaffold subunit A and catalytic subunit Ppg1. **a** Yeast two-hybrid analysis of the interaction between regulatory subunit MoB56, catalytic subunit Ppg1 and scaffold subunit PP2Aa. MoB56, Ppg1 and PP2Aa were inserted into vector pGADT7 and/or pGBKT7. BD-MoB56 and AD-Ppg1, BD-Ppg1 and AD-MoB56, BD-Ppg1 and AD-PP2Aa, BD-MoB56 and AD-PP2Aa were co-introduced into yeast Y2HGOLD strain, respectively, and then incubated on SD-Leu-Trp (as control) and SD-Leu-Trp-His (for selection) for 3–5 days. **b** Partial proteins precipitated with Ppg1-3Flag and identified by LC-MS/MS. **c** Co-immunoprecipitation assay shows that MoB56-3HA interacts with Ppg1-3Flag. A nuclear protein (predicted 85 kDa) fused 3Flag tag protein construct was used as a control

Co-IP eluate by the HA antibody, including three major bands whose assessed molecular weights were about 86, 75 and 71 kDa, respectively (Fig. 6c bottom). The three major bands were also detected in MoB56-GFP expressing complementary transformants but not in P131 and GFP-expressing transformants (Additional file 1: Figure S2c, d), suggesting that these bands are MoB56-specific. To understand how these bands of MoB56 with differing molecular sizes are produced, we performed the following two analyses. The first was to check whether they were due to phosphorylation modification since we previously reported that MoB56 has phosphorylation sites (Wang et al. 2017). Therefore, we added lambda protein phosphatase to the total protein extracts of a transformant expressing MoB56-3HA and MoPpg1-3Flag and the Ppg1-3Flag immunoprecipitate eluate to dephosphorylate MoB56. However, the dephosphorylation treatment of MoB56 did not change the banding pattern of MoB56-HA (Additional file 1: Figure S2a, b). We also treated the total protein extracts of a MoB56-GFP expressing complementary transformants with lambda protein phosphatase, three bands without size change were again detected by GFP antibody (Additional file 1: Figure S2c). Together, these results suggest that the multiple sizes of MoB56 are not attributed to phosphorylation modification.

Since B56 in mammal cells is known to have multiple variants originating from alternatively spliced transcripts (Ota et al. 2004) and alternative translation (Jin

et al. 2009), we then analyzed transcripts of MoB56 in the P131 mycelia (Li et al. 2021). The analysis revealed that there were at least five alternative transcripts of MoB56 in the mycelia (Fig. 7a). These distinct transcripts can encode two MoB56 variants with 670 amino acids, two MoB56 variants with 647 amino acids and one MoB56 variant with 330 amino acids, and their theoretical molecular weights are 76.1, 73.7 and 38.8 kDa, respectively (Fig. 7b and Additional file 1: Figure S3). We thus suppose that the 75 and 71 kDa proteins of MoB56 may be originated from the 670 and 647 amino acid-encoding transcripts, respectively. For the 86 kDa MoB56 band, which is about 11 kDa bigger than the theoretical molecular weights of products encoded by the 670 and the 647 amino acid-encoding transcripts, we suppose that it may be due to sumoylation modification of the proteins translated from the two transcripts or one of them. Further analysis with the GPS-SUMO program predicted two potential sumoylation sites with high confidence that lay at the positions of K6 and K405 (Zhao et al. 2014), suggesting that MoB56 is possibly modified by sumoylation.

To understand how MoB56 and Ppg1 are assembled into a protein complex, we further performed Y2H assays, showing that PP2Aa could interact with both MoB56 and MoPpg1 (Fig. 6a). This result indicates that the scaffold subunit PP2Aa ties MoB56 with MoPpg1 to generate a protein phosphatase complex.

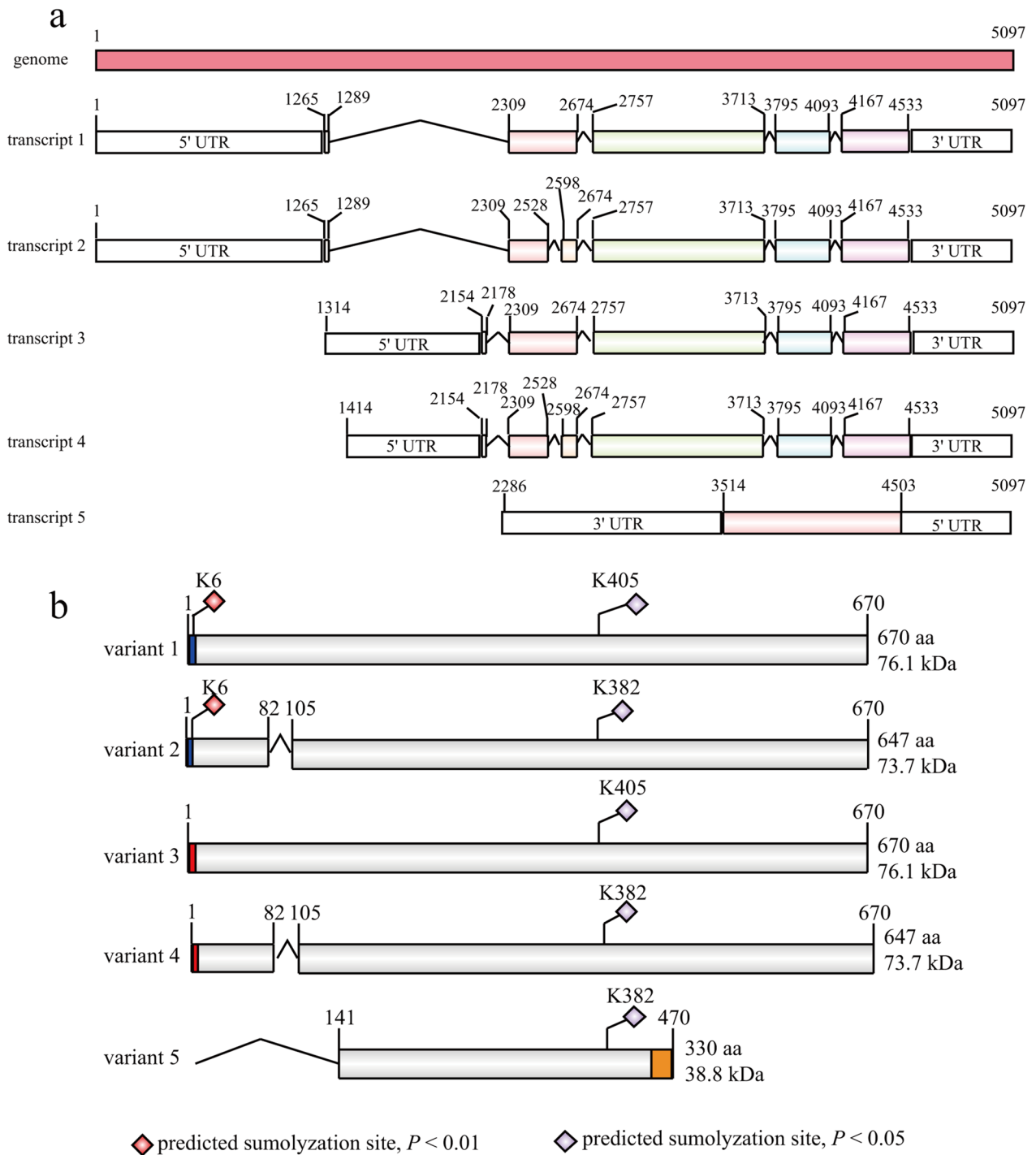


Fig. 7 Schematic diagrams showing alternatively spliced transcripts encoding distinct MoB56 variants in *Magnaporthe oryzae*. **a** Five transcripts of MoB56 identified in P131 mycelia. The RNA-seq data previously reported by Li et al. (2021) were used to identify the transcripts originating from alternative splicing of MoB56. Intron retention events were found in transcript 1 and transcript 3. Curved lines indicate introns spliced from the transcripts, and exons are represented by color-filled boxes with numbers that indicate start and end positions. The 5' and 3' untranslated regions are represented with blank boxes. **b** Deduced variants of MoB56 from transcripts in **a**. Colored boxes indicate the amino acid sequences different between the variants. Curved lines with numbers indicate the amino acid sequences absent from the variant as compared with others. Diamonds with numbers indicate potential sites of sumoylation

Discussion

PP2A is a major serine/threonine protein phosphatase family in eukaryotes (Janssens and Goris 2001; Virshup and Shenolikar 2009; Offley and Schmidt 2019). However, the function and regulatory mechanism of the PP2A holoenzyme complex in the fungal pathogen *M. oryzae* are largely unknown. Previously, whole genome sequencing revealed that *M. oryzae* carries one scaffold subunit, three regulatory subunits and one typical catalytic subunit PP2Ac, with one PP2A-like catalytic subunit MoPpg1 (Dean et al. 2005; Xue et al. 2012). Up to date, except for MoPpg1 (Du et al. 2013), the other subunits have not been functionally characterized in *M. oryzae*. In the present study, we showed that deleting *MoB56* in *M. oryzae* resulted in severe defects in vegetative growth, conidiation, septum formation and conidial morphology, indicating that MoB56 plays a crucial role in vegetative growth and asexual development. These defects of the $\Delta mob56$ mutant are similar to the phenotypes observed in the deletion mutants of the orthologous gene reported in yeast and other fungi. In *Candida albicans*, CaRts1 regulates hyphal growth, morphogenesis and septin ring organization (Han et al. 2019). In *Aspergillus nidulans*, the deletion mutant of the B56 regulatory subunit $\Delta parA$ displayed a shorter distance between two septa (Zhong et al. 2014). In addition, we showed that the conidia size of $\Delta mob56$ was smaller than the wild-type (Fig. 3a). In *S. cerevisiae*, ScRts1, the B56 regulatory subunit, is known to regulate the cell size via controlling TORC2 signaling (Lucena et al. 2018). These lines of evidence indicate that the B56 subunits of PP2A phosphatases in fungi are functionally conserved for controlling vegetative growth, conidial morphology and septum formation.

To date, reports on the B56 regulatory subunits in plant pathogenic fungi are limited. Only in *E. verticillioides*, the B56 regulatory subunit is known to be important for virulence (Shin et al. 2013). Our results showed that $\Delta mob56$ failed to penetrate the barley and rice leaves and expand in the wounded leaves (Fig. 4a, b). Further, $\Delta mob56$ rarely forms appressorium (Fig. 4g), and no penetration was observed in the barley leaves (Fig. 4c). These results indicate that the MoB56 regulatory subunit is essential to the pathogenicity of *M. oryzae*, providing a potential target for screening or designing agrochemicals to control this devastating fungal pathogen. Therefore, it will be interesting to investigate why the B56 regulatory subunits in different fungi play distinct roles in their pathogenicity. Sequence alignment of B56 subunits from yeasts, mammals and plants showed that B56 subunits are highly conserved at the HEAT-like domains but are diversified at both the N- and C-termini (Fig. 1a and Additional file 1: Figure S1). Further studies are therefore required to verify whether the N- and/or C-terminal divergency of

the B56 subunits is critical to the difference in the pathogenicity between different pathogenic fungi.

A major question of PP2A phosphatase in plant pathogenic fungi is how PP2A holoenzymes assemble and catalyze the diverse substrates with exquisite specificity. It has been known that the regulatory subunit Cdc55 and Rts1 in yeasts and some filamentous model fungi could associate with the scaffold subunit A and typical catalytic subunit to generate holoenzyme in vivo (Wei et al. 2001; Shomin-Levi and Yarden 2017; Han et al. 2019). However, besides the typical catalytic subunit C, fungi contain a PP2A-like catalytic subunit named Ppg1 in *S. cerevisiae* (Posas et al. 1993). The relationship between Ppg1 and the regulatory subunits B55 and B56 has not been reported. In the present study, we found that MoB56 interacts with the scaffold subunit A to generate a protein complex with Ppg1 in mycelial cells (Fig. 6). This is the first report for revealing the relationship of B56 subunit and Ppg1 in fungi and deciphering how the Ppg1 PP2A-like phosphatase regulates fungal pathogenicity. However, further investigation is required to identify substrates of the MoB56-Ppg1 complex, which are keys to understanding the mechanisms of how a Ppg1 PP2A-like phosphatase regulates fungal pathogenicity.

In this study, we also detected multiple isoforms of MoB56 in the mycelia of *M. oryzae*. Through analyzing RNA-seq data, we revealed that some of the isoforms may be originated from alternative splicing of the transcripts of *MoB56* (Fig. 7). In addition, we found that sumoylation may contribute to the isoform production of MoB56. These findings provide important information for further elucidating how MoB56 and its related phosphatases regulate mycelial growth, conidiation, septation and pathogenicity. However, further investigation is required to reveal how the individual isoforms regulate distinct phenotypes, verify whether MoB56 is sumoylated and identify which residue is sumoylated. It will be particularly interesting to investigate which of the isoforms and how the isoform regulates fungal pathogenicity and septum formation.

Conclusion

PP2A is usually heterotrimeric, consisting of a catalytic subunit C and a scaffolding subunit A associated with a third variable regulatory subunit B. The rice blast fungus *M. oryzae* has one scaffold subunit, three regulatory subunits and one typical catalytic subunit PP2Ac, with one PP2A-like catalytic subunit MoPpg1. However, except for MoPpg1, the other subunits have yet to be functionally characterized. In the present study, we found that MoB56 is important for septum formation, growth and conidia morphology and is essential for fungal pathogenicity. MoB56 is widely distributed in the cytoplasm and forms

a dot-like structure at the center of the septum. Further, we revealed that MoB56 forms a complex with the A subunit and MoPpg1 via direct interaction with subunit A. This is the first report revealing the relationship of the B56 subunit with Ppg1 in fungi. Taken together, this study provides information for understanding how the regulatory subunit B56 of PP2A regulates fungal pathogenicity and for the control of rice blast disease.

Methods

Fungal strains, growth conditions and DNA analysis

Storage, maintenance and growth of the *M. oryzae* strains, and nucleic acid extraction were carried out as described previously (Wang et al. 2017).

MoB56 gene replacement, mutant verification and complementation

To generate the *MoB56* gene replacement construct pKOV-MoB56, a 1.3-kb upstream fragment (primers MoB56_LF and MoB56_LR) and a 1.5-kb downstream fragment (primers MoB56_RF1/MoB56_RR1 and MoB56_RF2/MoB56_RR2) of the gene were independently amplified and cloned into the *SpeI*-*Bam*HI and *Hind*III-*Xho*I sites of pKOV21. After linearization with *Not*I, pKOV-MoB56 was transformed into the wild-type strain P131 to generate *MoB56* deletion mutants, which were first identified by PCR and then confirmed by Southern blot hybridization. Genomic DNAs of the *MoB56* mutant and wild-type strain P131 were digested by *Sal*I, and the 1.5-kb downstream fragment was used as a probe for detecting an expected 3.6 kb and an expected 10.2 kb digested fragment in genomic DNAs of P131 and the Δ *mob56* mutant, respectively. To generate the *MoB56*-GFP complementary construct pGTN-MoB56, the *MoB56* with 1.4-kb upstream sequence was amplified and cloned into the pGTN vector that contained the eGFP-TrpC terminator. The complementary construct was then transferred into the Δ *mob56* to generate complementary strains that were selected by neomycin resistance. Primers used to contrive the vectors are listed in Additional file 2: Table S1.

Protoplasts were isolated and transformed as described (Yang et al. 2010). Media were supplemented with 250 μ g/mL hygromycin B (Roche, NJ, USA) or 400 μ g/mL neomycin (Ameresco, OH, USA) to select hygromycin- or neomycin-resistant transformants.

Growth rate and conidiation measurement

The diameters of colonies were measured from five-day-old cultures grown on oatmeal tomato agar (OTA) as described previously (Yang et al. 2010). Conidia were

harvested from the OTA plates after 7 days at 28°C to estimate conidiation.

Infection assay

Conidial suspension adjusted to 4×10^4 conidia/mL in distilled water containing 0.025% Tween-20 was dropped on seven-day-old barley seedlings. Lesion formation was surveyed five days after inoculation on barley seedlings. For wound inoculation, the wounded rice leaves were inoculated with colony blocks and assessed for lesion formation five days after inoculation.

Appressorium formation and penetration assay

The conidial suspension was spotted onto hydrophobic coverslips and followed different inoculation times at 28°C for epifluorescence microscopy and calculated the appressorium formation rate (12 hpi), and dropped onto barley leaves following 24 hpi inoculation for penetration assay and subcellular localization observation.

Epifluorescence microscopy and CFW staining

M. oryzae cells, including hyphae, conidia and appressorium expressing GFP fluorescent fusion proteins were incubated under appropriate conditions. The Nikon 90i microscope was used for epifluorescence microscopy. For CFW staining, mycelia were stained with 20 μ g/mL for 1 min in the dark, and conidia were stained for 30 min in the dark.

Yeast two-hybrid (Y2H) assay

To generate bait and prey vectors for yeast two-hybrid assay, the coding sequence of *MoPpg1* was amplified with the MoPpg1-BD_F and MoPpg1-BD_R primers and cloned into the *Eco*RI-*Pst*I site of the pGBDK7 vector (Clontech, CA, USA). All the other bait and prey vectors were constructed by cloning coding sequences into the *Nde*I-*Eco*RI site of the pGBDK7 vector and/or the pGADT7. Primers used to contrive the vectors are listed in Additional file 2: Table S1.

Constructs of BD-MoB56 and AD-Ppg1, BD-Ppg1 and AD-MoB56, BD-Ppg1 and AD-PP2Aa, BD-MoB56 and AD-PP2Aa were co-introduced into yeast Y2HGold strain (Clontech), respectively, and then incubated on SD-Leu-Trp plates (as control) and SD-Leu-Trp-His plates to test protein-protein interactions.

Co-immunoprecipitation (Co-IP) assay

To generate the MoPpg1-3Flag and MoB56-HA vectors for Co-IP assay, *MoB56* with 1.5-kb upstream sequence was amplified and cloned into the YIP105 vector that contained the HA tag and TrpC terminator, and *MoPpg1* with 1.4-kb upstream sequence was amplified and cloned into the YIP101 vector that contained

the 3Flag tag and TrpC terminator. The MoPpg1-3Flag and MoB56-HA constructs were co-transferred into the wild-type strain P131 to generate co-expression strains. Primers used to contrive the vectors are listed in Additional file 2: Table S1. The transformants resistant to neomycin and glufosinate were isolated. Total proteins were extracted from the transformants using protein lysis buffer (50 mM Tris HCl pH 7.5, 150 mM NaCl, 1 mM EDTA, 1% Triton X-100, protease inhibitor cocktail (Sigma, MO, USA)) and incubated with anti-Flag Magnetic beads (MedChemExpress, China) for 2 h, followed by washing the beads with a cold washing buffer (10 mM Tris HCl pH 7.5, 150 mM NaCl, 0.5 mM EDTA) four times. The proteins bound to the beads were eluted and denatured by water boiling with a protein loading buffer. A strain from another study that expressed a nuclear protein fused 3Flag tag was used as a negative control. Total protein extracted from the strain and proteins extracted from the strain that contains YIP105-MoB56-HA construct alone were co-incubated with anti-Flag Magnetic beads as mentioned above. The 3Flag fused control protein failed to pull MoB56-HA down. The eluted proteins that co-immunoprecipitated Ppg1-3Flag and control-3Flag were detected by anti-Flag antibody (Sigma, MO, USA) and anti-HA antibody (Roche, Mannheim, Germany).

Abbreviations

CFW	Calcofluor white
Co-IP	Co-immunoprecipitation
OTA	Oatmeal tomato agar
PP2A	Protein phosphatase 2A
STRIPAK complex	Striatin-interacting phosphatase and kinase complex
TAP-MS	Tandem affinity purification and mass spectrometry
Y2H	Yeast two-hybrid assay

Supplementary Information

The online version contains supplementary material available at <https://doi.org/10.1186/s42483-023-00165-1>.

Additional file 1: Figure S1. Sequence alignment of the regulatory B56 subunits across species. **Figure S2.** Western blot assay for detecting band shift patterns of MoB56 with and without protein phosphatase treatment. **Figure S3.** Sequence alignment of the five MoB56 variants identified in P131.

Additional file 2: Table S1. Primers used in this study.

Acknowledgements

We thank Professor Vijai Bhaduria in China Agricultural University for his critical reading and comments.

Authors' contributions

RW and YP designed experiments; RW, RZ, DC, YJ, YY, WZ, LQ and LX performed the experiments and analyzed the data; RW and YP wrote the manuscript. All authors read and approved the final manuscript.

Funding

This work was supported by the National Natural Science Foundation of China (Grant No. 32000104), China Agricultural Research System (Grant No. CARS-01-36 and CARS-01-44), and China Postdoctoral Science Foundation (Grant No. 2019M650905) for the design of the study and collection, analysis and interpretation of data.

Availability of data and materials

Not applicable.

Declarations

Ethics approval and consent to participate

Not applicable.

Consent for publication

Not applicable.

Competing interests

The authors declare that they have no competing interests.

Received: 16 October 2022 Accepted: 6 February 2023

Published online: 21 March 2023

References

- Beier A, Teichert I, Krisp C, Wolters DA, Kuck U. Catalytic subunit 1 of protein phosphatase 2A is a subunit of the STRIPAK complex and governs fungal sexual development. *MBio*. 2016;7(3):e00870–16. [https://doi.org/10.1016/S0021-9258\(17\)34009-7](https://doi.org/10.1016/S0021-9258(17)34009-7).
- Booker MA, DeLong A. Atypical protein phosphatase 2A gene families do not expand via paleopolyploidization. *Plant Physiol*. 2017;173(2):1283–300. <https://doi.org/10.1104/pp.16.01768>.
- Cohen PTW. Phosphatase families dephosphorylating serine and threonine residues in proteins. In: Bradshaw RA, Dennis EA, editors. *Handbook of Cell Signaling*. 2nd ed. San Diego: Academic; 2010. pp. 659–75. <https://doi.org/10.1016/B978-0-12-374145-5.00085-1>.
- Dean RA, Talbot NJ, Ebbole DJ, Farman ML, Mitchell TK, Orbach MJ, et al. The genome sequence of the rice blast fungus *Magnaporthe grisea*. *Nature*. 2005;434(7036):980–6. <https://doi.org/10.1038/nature03449>.
- Dean R, Van Kan JA, Pretorius ZA, Hammond-Kosack KE, Di Pietro A, Spanu PD, et al. The top 10 fungal pathogens in molecular plant pathology. *Mol Plant Pathol*. 2012;13(4):414–30. <https://doi.org/10.1111/j.1364-3703.2011.00783.x>.
- Dobbelaere J, Gentry MS, Hallberg RL, Barral Y. Phosphorylation-dependent regulation of septin dynamics during the cell cycle. *Dev Cell*. 2003;4(3):345–57. [https://doi.org/10.1016/S1534-5807\(03\)00061-3](https://doi.org/10.1016/S1534-5807(03)00061-3).
- Du Y, Shi Y, Yang J, Chen X, Xue M, Zhou W, et al. A serine/threonine-protein phosphatase PP2A catalytic subunit is essential for asexual development and plant infection in *Magnaporthe oryzae*. *Curr Genet*. 2013;59(1–2):33–41. <https://doi.org/10.1007/s00294-012-0385-3>.
- Ghosh A, Servin JA, Park G, Borkovich KA. Global analysis of serine/threonine and tyrosine protein phosphatase catalytic subunit genes in *Neurospora crassa* reveals interplay between phosphatases and the p38 mitogen-activated protein kinase. *G3*. 2014;4(2):349–65. <https://doi.org/10.1534/g3.113.008813>.
- Han Q, Pan C, Wang Y, Wang N, Wang Y, Sang J. The PP2A regulatory subunits, Cdc55 and Rts1, play distinct roles in *Candida albicans*' growth, morphogenesis, and virulence. *Fungal Genet Biol*. 2019;131:103240. <https://doi.org/10.1016/j.fgb.2019.103240>.
- Healy AM, Zolnierowicz S, Stapleton AE, Goebel M, DePaoli-Roach AA, Pringle JR. CDC55, a *Saccharomyces cerevisiae* gene involved in cellular morphogenesis: identification, characterization, and homology to the B subunit of mammalian type 2A protein phosphatase. *Mol Cell Biol*. 1991;11(11):5767–80. <https://doi.org/10.1128/mcb.11.11.5767-5780.1991>.
- Hunter T. Protein kinases and phosphatases: the yin and yang of protein phosphorylation and signaling. *Cell*. 1995;80(2):225–36. [https://doi.org/10.1016/0092-8674\(95\)90405-0](https://doi.org/10.1016/0092-8674(95)90405-0).

- Janssens V, Goris J. Protein phosphatase 2A: a highly regulated family of serine/threonine phosphatases implicated in cell growth and signalling. *Biochem J*. 2001;353(3):417–39. <https://doi.org/10.1042/0264-6021:3530417>.
- Jiang W, Hallberg RL. Isolation and characterization of par1(+) and par2(+): two *Schizosaccharomyces pombe* genes encoding B' subunits of protein phosphatase 2A. *Genetics*. 2000;154(3):1025–38. <https://doi.org/10.1093/genetics/154.3.1025>.
- Jin Z, Shi J, Saraf A, Mei W, Zhu GZ, Strack S, et al. The 48-kDa alternative translation isoform of PP2A:B56epsilon is required for wnt signaling during midbrain-hindbrain boundary formation. *J Biol Chem*. 2009;284(11):7190–200. <https://doi.org/10.1074/jbc.M807907200>.
- Kiely M, Kiely PA. PP2A: the wolf in sheep's clothing? *Cancers*. 2015;7(2):648–69. <https://doi.org/10.3390/cancers7020648>.
- Kück U, Beier AM, Teichert I. The composition and function of the striatin-interacting phosphatases and kinases (STRIPAK) complex in fungi. *Fungal Genet Biol*. 2016;90:31–8. <https://doi.org/10.1016/j.fgb.2015.10.001>.
- Li Z, Yang J, Peng J, Cheng Z, Liu X, Zhang Z, et al. Transcriptional landscapes of long non-coding RNAs and alternative splicing in *Pyricularia oryzae* revealed by RNA-Seq. *Front Plant Sci*. 2021;12:723636. <https://doi.org/10.3389/fpls.2021.723636>.
- Lucena R, Alcaide-Gavilán M, Schubert K, He M, Domnauer MG, Marquer C, et al. Cell size and growth rate are modulated by TORC2-dependent signals. *Curr Biol*. 2018;28(2):196–210.e4. <https://doi.org/10.1016/j.cub.2017.11.069>.
- Offley SR, Schmidt MC. Protein phosphatases of *Saccharomyces cerevisiae*. *Curr Genet*. 2019;65(1):41–55. <https://doi.org/10.1007/s00294-018-0884-y>.
- Ota T, Suzuki Y, Nishikawa T, Otsuki T, Sugiyama T, Irie R, et al. Complete sequencing and characterization of 21,243 full-length human cDNAs. *Nat Genet*. 2004;36(1):40–5. <https://doi.org/10.1038/ng1285>.
- Posas F, Clotet J, Muns MT, Corominas J, Casamayor A, Ariño J. The gene PPG encodes a novel yeast protein phosphatase involved in glycogen accumulation. *J Biol Chem*. 1993;268(2):1349–54. [https://doi.org/10.1016/S0021-9258\(18\)54082-5](https://doi.org/10.1016/S0021-9258(18)54082-5).
- Qiu M, Li Y, Ye W, Zheng X, Wang Y. A CRISPR/Cas9-mediated in situ complementation method for *Phytophthora sojae* mutants. *Mol Plant Pathol*. 2021;22(3):373–81. <https://doi.org/10.1111/mpp.13028>.
- Shi Y. Serine/threonine phosphatases: mechanism through structure. *Cell*. 2009;139(3):468–84. <https://doi.org/10.1016/j.cell.2009.10.006>.
- Shin JH, Kim JE, Malapi-Wight M, Choi YE, Shaw BD, Shim WB. Protein phosphatase 2A regulatory subunits perform distinct functional roles in the maize pathogen *Fusarium verticillioides*. *Mol Plant Pathol*. 2013;14(5):518–29. <https://doi.org/10.1111/mpp.12023>.
- Shomin-Levi H, Yarden O. The *Neurospora crassa* PP2A regulatory subunits RGB1 and B56 are required for proper growth and development and interact with the NDR kinase COT1. *Front Microbiol*. 2017;8:1694. <https://doi.org/10.3389/fmicb.2017.01694>.
- Shu Y, Yang H, Hallberg E, Hallberg R. Molecular genetic analysis of Rts1p, a B' regulatory subunit of *Saccharomyces cerevisiae* protein phosphatase 2A. *Mol Cell Biol*. 1997;17(6):3242–53. <https://doi.org/10.1128/MCB.17.6.3242>.
- Sneddon AA, Cohen PT, Stark MJ. *Saccharomyces cerevisiae* protein phosphatase 2A performs an essential cellular function and is encoded by two genes. *EMBO J*. 1990;9(13):4339–46. <https://doi.org/10.1002/j.1460-2075.1990.tb07883.x>.
- van Zyl W, Huang W, Sneddon AA, Stark M, Camier S, Werner M, et al. Inactivation of the protein phosphatase 2A regulatory subunit results in morphological and transcriptional defects in *Saccharomyces cerevisiae*. *Mol Cell Biol*. 1992;12(11):4946–59. <https://doi.org/10.1128/mcb.12.11.4946-4959.1992>.
- Vargas-Muñiz JM, Renshaw H, Richards AD, Waite G, Soderblom EJ, Moseley MA, et al. Dephosphorylation of the core septin, AspB, in a protein phosphatase 2A-dependent manner impacts its localization and function in the fungal pathogen *aspergillus fumigatus*. *Front Microbiol*. 2016;7:997. <https://doi.org/10.3389/fmicb.2016.00997>.
- Virshup DM, Shenolikar S. From promiscuity to precision: protein phosphatases get a makeover. *Mol Cell*. 2009;33(5):537–45. <https://doi.org/10.1016/j.molcel.2009.02.015>.
- Wang RJ, Peng J, Li QX, Peng YL. Phosphorylation-mediated regulatory networks in mycelia of *Pyricularia oryzae* revealed by phosphoproteomic analyses. *Mol Cell Proteom*. 2017;16(9):1669–82. <https://doi.org/10.1074/mcp.M116.066670>.
- Wei H, Ashby DG, Moreno CS, Ogris E, Yeong FM, Corbett AH, et al. Carboxymethylation of the PP2A catalytic subunit in *Saccharomyces cerevisiae* is required for efficient interaction with the B-type subunits Cdc55p and Rts1p. *J Biol Chem*. 2001;276(2):1570–7. <https://doi.org/10.1074/jbc.M008694200>.
- Wilson WA, Wang Z, Roach PJ. Systematic identification of the genes affecting glycogen storage in the yeast *Saccharomyces cerevisiae*: implication of the vacuole as a determinant of glycogen level. *Mol Cell Proteom*. 2002;1(3):232–42. <https://doi.org/10.1074/mcp.m100024-mcp200>.
- Xue M, Yang J, Li Z, Hu S, Yao N, Dean RA, et al. Comparative analysis of the genomes of two field isolates of the rice blast fungus *Magnaporthe oryzae*. *PLoS Genet*. 2012;8(8):e1002869. <https://doi.org/10.1371/journal.pgen.1002869>.
- Yang J, Zhao XY, Sun J, Kang ZS, Ding SL, Xu JR, et al. A novel protein Com1 is required for normal conidium morphology and full virulence in *Magnaporthe oryzae*. *Mol Plant Microbe Interact*. 2010;23(1):112–23. <https://doi.org/10.1094/MPMI-23-1-0112>.
- Zhao Q, Xie Y, Zheng Y, Jiang S, Liu W, Mu W, et al. GPS-SUMO: a tool for the prediction of sumoylation sites and SUMO-interaction motifs. *Nucleic Acids Res*. 2014;42(1):W325–30. <https://doi.org/10.1093/nar/gku383>.
- Zhong GW, Jiang P, Qiao WR, Zhang YW, Wei WF, Lu L. Protein phosphatase 2A (PP2A) regulatory subunits ParA and PabA orchestrate septation and conidiation and are essential for PP2A activity in *aspergillus nidulans*. *Eukaryot Cell*. 2014;13(12):1494–506. <https://doi.org/10.1128/EC.00201-14>.

Ready to submit your research? Choose BMC and benefit from:

- fast, convenient online submission
- thorough peer review by experienced researchers in your field
- rapid publication on acceptance
- support for research data, including large and complex data types
- gold Open Access which fosters wider collaboration and increased citations
- maximum visibility for your research: over 100M website views per year

At BMC, research is always in progress.

Learn more biomedcentral.com/submissions

